INTERFERENCE SUPPRESSION USING PARASITIC RECONFIGURABLE APERTURE (RECAP) ANTENNAS

Rashid Mehmood and Jon W. Wallace*

Jacobs University Bremen
School of Engineering and Science
Campus Ring 1, 28759 Bremen, Germany
r.mehmood@ieee.org, wall@ieee.org

INTRODUCTION

Most of today's practical wireless systems are interference limited, meaning that the degree of spectral reuse possible is dictated by the size of the coverage area (or cell) and the degree of tolerable interference experienced at the cell edges. Much higher spectral reuse is possible with nodes that can control their radiation patterns to suppress and avoid interference, which is also the basis of spatial division multiple access (SDMA) techniques. A typical goal in interference-limited systems is to maximize the signal-to-interference ratio (SIR) of the nodes in the network. Although SIR minimization is possible with array signal processing, a drawback is the need for additional radio-frequency (RF) chains and digital signal processing (DSP) resources.

Reconfigurable antennas represent an attractive alternative to interference reduction with conventional array processing, since synthesis of pattern nulls can be performed with tunable analog components [1], [2] that are inexpensive and have low power consumption, reducing the overall cost of the system. The reconfigurable aperture (RECAP) antenna is an interesting concept that can be viewed as a generalization of reconfigurable antennas, potentially supporting applications such as beamforming, interference suppression, and frequency and bandwidth tuning with a single versatile architecture [3], [4]. A RECAP typically consists of a dense array of analog reconfigurable elements (REs), where each RE can have a number of reconfigurable states (RSs), which can be dynamically manipulated to change the characteristics of the aperture to suit the current application.

In [3], we considered the dependence of performance on RECAP complexity for a beamforming application, indicating the number of reconfigurable elements per wavelength that are needed to reach diminishing returns. This present work considers combined beamforming and null synthesis with RECAPs, with the goal of understanding what level and what type of RECAP complexity is required to provide high SIR in multi-user, interference limited scenarios, and observations are compared with the beamforming application in [3]. We also consider how the results scale as the number of required RECAP nulls increases, which is directly related to the number of interfering users and multipath directions in a practical scenario.

SIMULATION OF THE PARASITIC RECAP STRUCTURE

The structure considered in this work is depicted in Figure 1(a), consisting of a 9×9 square array of half-wave dipoles occupying area $1\lambda \times 1\lambda$ in the xy plane and height $\lambda/2$ in z, where the center element serves as an active feed and the other antennas are terminated with reconfigurable loads. Figure 1(b) shows a top view of the structure for a varying number of reconfigurable elements (N_{RE}). Note that although *planar* RECAPs are more practical for low-profile mobile devices, the dipole array is more convenient for initial theoretical studies since it is conceptually simple and efficient to simulate. Also, we have found that the trends seen in the parasitic dipole RECAP are very similar to those observed for planar RECAP structures [4]. In this work, the RSs are assumed to be tunable capacitances (practically fabricated with varactor diodes or tunable MEMs capacitors), which present an input reflection coefficient with a phase in the range of $0°$ to $-180°$ in response to the applied bias voltage.

In order to compute the radiation pattern and input impedance of the RECAP for a particular configuration of REs, a hybrid approach is used. First, full wave simulations are performed using the Numerical Electromagnetics Code (NEC), where for each simulation a single port (the feed or an RE site) is excited with a voltage source and all other ports are short-circuited, and the resulting port currents and radiation pattern are stored. Repeating this for all ports provides the input Y-parameter (admittance) matrix of the RECAP and the set of embedded short-circuit radiation patterns that completely characterize the array [4]. These quantities can then be converted to Z-parameter (impedance) or S-parameter quantities as is convenient for the analysis at hand. Second, network analysis can be applied to compute the radiation pattern and input impedance of the RECAP for arbitrary configuration of the REs and RSs. This procedure is orders of magnitude more efficient than unified full-wave simulations, since many 1000s of RECAP configurations are to be considered.

Since RECAPs with large complexity are considered, the number of RE combinations is too large in most cases for an exhaustive search, even with the efficient hybrid simulation technique. Therefore, in this work, a genetic algorithm (GA) is employed to find suitable solutions, which is equivalent to that presented in [4].
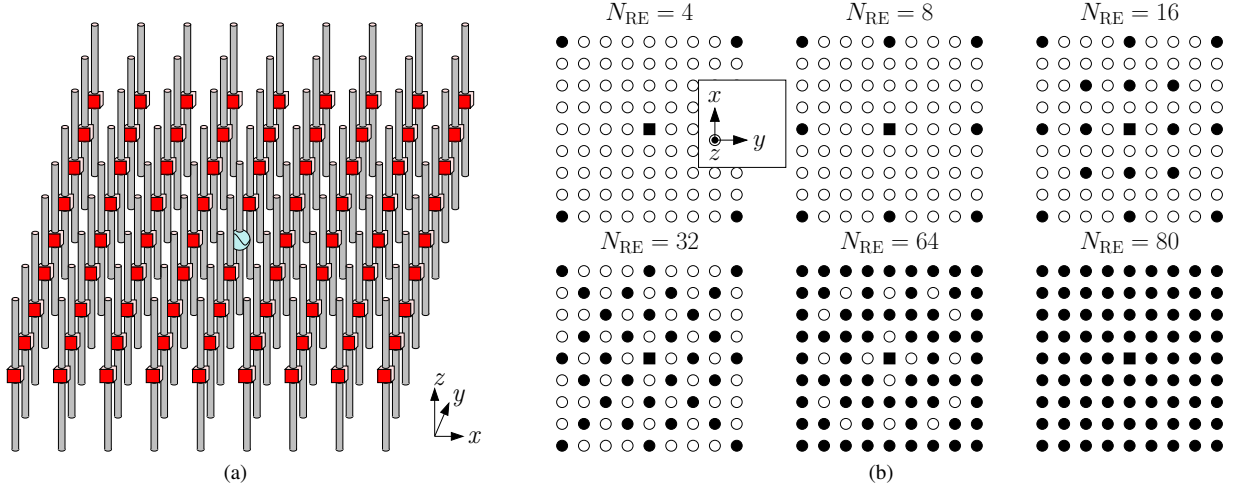
Fig. 1. RECAP structure consisting of a 9×9 dipole array, where N_{RE} elements are terminated with REs and the center element is the feed. In (a) a perspective view with $N_{\mathrm{RE}} = 80$ is shown. In (b) a top view is shown for configurations with different complexities, where RE-terminated elements are indicated with filled circles.

RECAP OPTIMIZATION

The performance goal considered in this paper is that of maximizing SIR, and note that for this study, only radiation in the azimuthal (xy plane) and vertical (θ-directed) polarization are considered. For the transmit case, the relative fraction of input power radiated into direction ϕ_i is given by

$$\mathrm{P}(\phi_i) = \max_{\mathbf{Z}_L}(1 - |\Gamma|^2)\frac{|E_\theta(\phi_i, \theta = \pi/2)|^2}{\sum_{n=1}^{N_A} |E_\theta(\phi_n, \theta = \pi/2)|^2}, \tag{1}$$

where $\mathbf{Z}_L$ is the diagonal impedance matrix with the RE impedances on the diagonal, and Γ and $E_\theta(\phi, \theta)$ are the input reflection coefficient and realized radiation pattern looking into the feed that depend implicitly on $\mathbf{Z}_L$. For the receive case, the same expression represents the relative amount of available power from direction ϕ_i that is delivered to the load. Thus, (1) can be used to consider either interference suppression (receive mode) or avoidance (transmit mode).

Assuming N_{int} interferers, where the ith interferer is at angle $\phi_{\mathrm{int},k}$, SIR for signal in direction ϕ_{main} with respect to the worst-case interferer for the receive mode is defined as

$$\rho' = \frac{P(\phi_{\mathrm{main}})}{\max_k[P(\phi_{\mathrm{int},k})]}, \tag{2}$$

which assumes that the available power from the interferers is equal to that of the desired user at angle ϕ_{main}. For GA optimization, the fitness of a particular configuration is chosen to be the SIR in (2) converted to dB. In the following analysis, the set of reconfigurable states is chosen to be uniformly distributed over the range of $[-180°, 0°]$. Additionally, when considering the effect of finite bandwidth, the center frequency of the RECAP is assumed to be $f_0 = 3$ GHz with a bandwidth of $W = 20$ MHz. The fitness for finite bandwidth is computed as average fitness for a single fixed state of the RECAP at the three frequencies $f = f_0 - W/2$, $f = f_0$, and $f = f_0 = W/2$.

Figure 2(a) shows the radiation pattern of the GA-optimized RECAP ($N_{\mathrm{RE}} = 80$, $N_{\mathrm{RS}} = 32$), where for each case a specific main beam direction (square) is chosen with 8 random desired null directions (circles). The result shows that the GA-optimized RECAP can find good solutions that transmit or receive high power in the desired direction and suppress power in the interferer directions. Figure 2(b) shows a result for finite bandwidth where the patterns at the two band edges and center frequency are individually plotted. The result shows that finite bandwidth makes the optimization more difficult since sharp nulls cannot be created at all frequencies and null directions simultaneously, but notice that the GA is still able to find solutions that keep the average interference low compared to the main beam.

PERFORMANCE VERSUS COMPLEXITY ANALYSIS

Figure 3(a) plots the convergence of the GA for $N_{\mathrm{RE}} = 32$ and increasing N_{RS}. The curves were obtained by averaging the results (in dB) for 4 interferers from 10 random configurations of angles with 5 runs of the GA per angle. The results show that for a fixed number of reconfigurable elements, adding more states helps in terms of achieving higher SIR, but that performance begins to saturate near $N_{\mathrm{RS}} = 16$. Figure 3(b) shows the convergence of the GA for $N_{\mathrm{RS}} = 32$ and an increasing number of reconfigurable elements, where the case of 8 interferers is analyzed. The results show
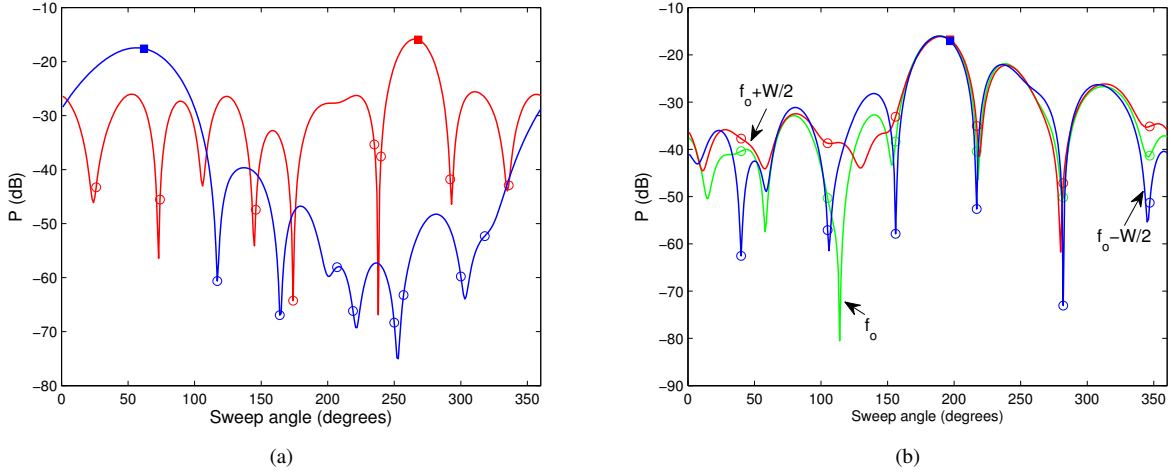
Fig. 2. Synthesized patterns of GA-optimized RECAP for SIR maximization, where the main beam direction and desired nulls are shown with a square and circles, respectively: (a) Single-frequency solution for $N_{\mathrm{RE}} = 80$, $N_{\mathrm{RS}} = 32$ with a main beam at $\phi_{\mathrm{main}} = 268°$ and $\phi_{\mathrm{main}} = 62°$, (b) finite bandwidth optimization with $N_{\mathrm{RE}} = 64$, $N_{\mathrm{RS}} = 32$, and $\phi_{\mathrm{main}} = 197°$, where patterns are shown for center frequency and band edges.
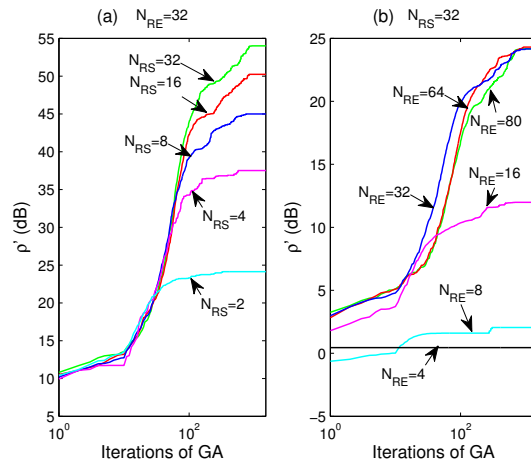

Fig. 3. Convergence in ρ' using the GA for (a) a fixed number of reconfigurable elements ($N_{\mathrm{RE}} = 32$) where multiple curves show increasing N_{RS} (states per RE) with 4 interferers, and (b) a fixed number of reconfigurable states ($N_{\mathrm{RS}} = 32$) where multiple curves show increasing N_{RE} with 8 interferers.

that for a fixed high number of RSs, adding REs increases performance dramatically until an abrupt saturation point at $N_{\mathrm{RE}} = 32$. Note that in all cases, additional complexity does not appear to hinder the rate of convergence of the GA.

Figure 4 allows us to study the effect of RECAP complexity in more detail by plotting the final SIR value obtained by the GA for different numbers of interferers (desired null directions). Each solid curve shows the SIR performance for a fixed value of N_{RE} where points on each curve are for increasing values of $N_{\mathrm{RB}} = \log_2(N_{\mathrm{RS}})$. The curves are positioned so that SIR performance is plotted with respect to total complexity of the RECAP ($N_{\mathrm{RE}}N_{\mathrm{RB}}$), allowing assessment of whether N_{RE} or N_{RS} is more important for improving performance.

Figures 4(a)-4(c) show the result for different numbers of nulls for optimization of the RECAP at a single frequency, and a number of observations can be made. We generally see that the dependence of performance on complexity can be divided into three regions: 1) For low complexity ($N_{\mathrm{RE}}N_{\mathrm{RB}}$ small), the performance depends more strongly on N_{RE} than N_{RS}, or in other words, more dense sampling of the aperture is more important than having finer phase tunability of the REs, which was similar to the beamforming application in [3]. 2) For medium complexity, the different curves begin to overlap, meaning that only total complexity is important and that both finer sampling of the aperture and finer phase tunability give about equal performance increase. This was also seen for high complexity in the beamforming application. 3) For high complexity, a point is reached where performance actually drops with higher N_{RE} but increases with N_{RS}. This means that when the aperture is sufficiently sampled, only additional phase tunability gives a significant performance increase, not more dense sampling of the aperture. Note that this final region was not seen for beamforming.
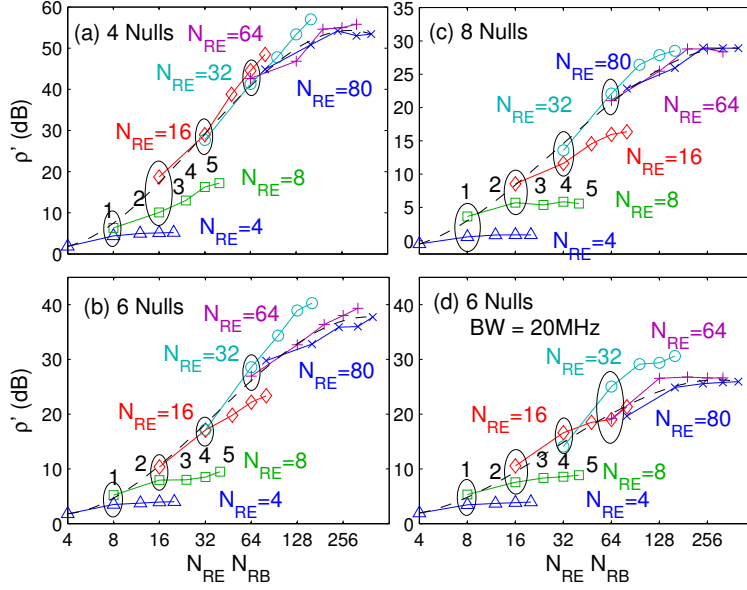
Fig. 4. Final ρ' fitness versus RECAP complexity for various numbers of interferers (desired nulls). Numbers 1-5 above curves show N_{RB} values (same pattern used but not labeled in other curves). The dashed line is a fitted cubic Bezier curve showing the overall trend. The circled points compare different solutions having equal complexity.

As the number of nulls is increased from 4 to 6 to 8 in Figures 4(a)-4(c), we first observe that the curves are becoming flatter, which means that sufficient spatial sampling becomes increasingly important in Region 1 (low complexity) and that the onset of Region 2 is pushed to higher complexity values. Second, we see that although trends are similar as more nulls are required, the absolute performance of all curves is reduced (note the change of the y scale for the different plots). This reduced performance suggests a fundamental limitation in null synthesis due to the fixed $1\lambda \times 1\lambda$ aperture size, or possibly difficulty of the GA in finding solutions for very high complexity.

The effect of optimizing over a finite bandwidth can be seen by comparing Figures 4(b) and 4(d). For low complexity (Region 1), there appears to be no change due to finite bandwidth. For high complexity, however, the performance is degraded significantly, and we see that the role of higher N_{RS} in Region 3 appears to be more important. In all cases, the level of complexity required for near peak performance for SIR maximization occurs near a total complexity of $N_{RE}N_{RB} = 128$, which can be accomplished with 8 elements per wavelength ($N_{RE} = 64$) and $N_{RS} = 4$ states per RE.

The effect of REs with loss has also been considered in this work, where simulations indicate that having a series resistance of up to 5Ω does not cause any significant change in the performance curves, even at high complexity, which is somewhat different from the results for beamforming in [3]. This should be expected, however, because for this interference suppression application, loss is less critical, since both signal and interference will be reduced by RE loss, whereas for the beamforming application signal is reduced by RE loss and noise remains constant.

CONCLUSION

In this work signal-to-interference ratio enhancement with RECAPs in the presence of a variable number of interferers was analyzed. SIR performance saturates at a total complexity of approximately $N_{RE}N_{RB} = 128$ (8 REs per wavelength and 4 RSs per element). It was observed that for lower N_{RE}, increasing N_{RE} is more beneficial as compared to increasing N_{RS}. However when the aperture is sufficiently sampled (around $N_{RE}=32$) increasing N_{RS} may be more beneficial than increasing N_{RE}, especially in the case when there are more interferers or a finite bandwidth is considered.

REFERENCES

[1] G. H. Huff, J. Feng, S. Zhang, G. Cung, and J. T. Bernhard, "Directional reconfigurable antennas on laptop computers: Simulation, measurement and evaluation of candidate integration positions," *IEEE Transactions on Antennas and Propagation*, vol. 52, no. 12, pp. 3220–3227, 2004.
[2] S. Nikolaou, R. Bairavasubramanian, J. Lugo, C., I. Carrasquillo, D. C. Thompson, G. E. Ponchak, J. Papapolymerou, and M. M. Tentzeris, "Pattern and frequency reconfigurable annular slot antenna using pin diodes," *IEEE Transactions on Antennas and Propagation*, vol. 54, no. 2, pp. 439–448, 2006.
[3] R. Mehmood and J. W. Wallace, "Diminishing returns with increasing complexity in reconfigurable aperture antennas," *IEEE Antennas and Wireless Propagation Letters*, vol. 9, pp. 299–302, 2010.
[4] R. Mehmood and J. W. Wallace, "Exploring beamforming performance versus complexity in reconfigurable aperture antennas," in *Proc. Int Smart Antennas (WSA) ITG Workshop*, pp. 383–389, 2010.